Chapter X
Mass-2-Spring (M2K) Systems

X.1 A Brief Introduction

Here we are considering a mass situated on a horizontal (perhaps frictionless) plane tethered to two supports as shown below, the distance between the supports is *2d*. We are primarily interested in *transverse* oscillations of the mass. There are two possible stable positions of the mass. The first (a) is where the unstretched length of the spring L_0 is greater than *d*, so if we start with a horizontal arrangement, then the springs start off in compression. The horizontal arrangement is now unstable, so the mass moves up (or down) as shown in Fig.1(a). There are two key *geometrical* parameters in this system, L_0 and *d*; we shall often take L_0 as our independent variable in discussions and experiments.

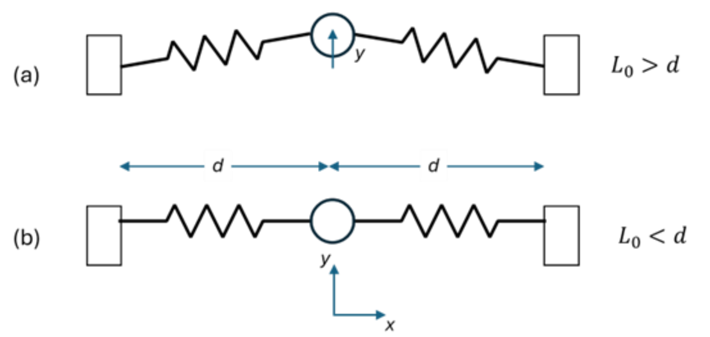

Figure 1. Top-down view of mass on springs showing two initial stable equilibria (a) springs start of in compression and (b) in tension.

If we start off with the unstretched length less than *d* ($L_0 < d$) then the springs start off in tension, so the arrangement Fig.1(b) is stable.

X.2 The Monostable solution

X.2.1 Equation of Motion and expected Frequencies

Here we are considering the situation Fig1(b) above, and we wish to establish the equation of motion of the mass (ordinary differential equation, ODE). This is straightforward; we resolve the forces exerted by the springs on the mass in the y-direction, shown in Fig.2 where the mass has been given an upward displacement *y*.

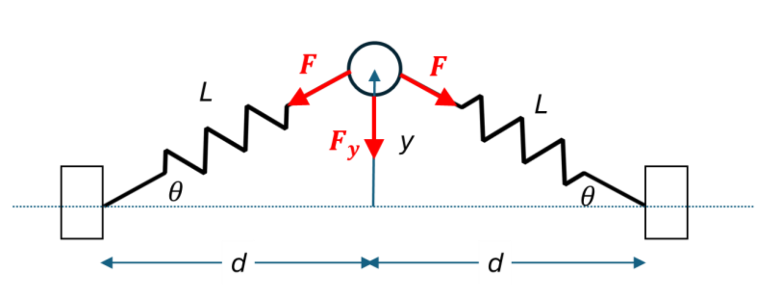

Figure 2. Springs initially in tension with a transverse displacement.

Consider one spring which is in tension. Since the unstretched length was L_0 and its current length is L then the force F in the spring is just

$$F = -k(L - L_0) \qquad (1)$$

So the downward force is

$$F_y = -k(L - L_0)\sin\theta \qquad (2)$$

The total downward force becomes

$$F_y = -2k((y^2 + d^2)^{\frac{1}{2}} - L_0)\frac{y}{(y^2 + d^2)^{\frac{1}{2}}}$$

$$= -2k\left[1 - \frac{L_0}{(y^2 + d^2)^{\frac{1}{2}}}\right]y \qquad (3)$$

Clearly this force is in general not proportional to displacement y so we do not expect harmonic motion. However, it is useful to sketch the form of this force for various values of L_0. Remember that $L_0 < d$ so we choose three values of L_0, one close to d, one close to zero and one in between. The results are shown in Fig.3 For small initial spring length L_0 when the spring is in place it is taut, the force is almost linear, and of course is restoring. When L_0 is close to d so the spring is not at all taut when in place, the force is dominated by the nonlinearity; close to the origin it has little stiffness which grows as the spring is stretched. This is definitely non-linear behaviour. The intermediate case is a mix of linear and nonlinear behaviour.

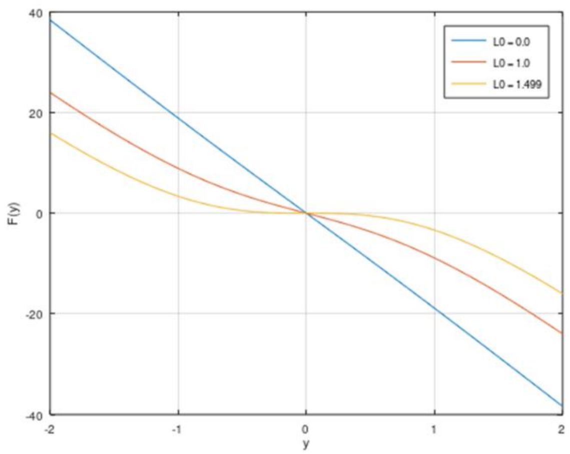

Figure 3. Behaviour of restoring force with initial displacement y for various values of initial spring length L_0.

In general, the force is not proportional to displacement so we do not expect harmonic motion, in general. However for small displacement where $y \ll d$ the above expression simplifies to

$$F = -2k\left[1 - \frac{L_0}{d}\right]y \qquad (4)$$

And so we expect harmonic motion with

$$\omega^2 = \frac{-dF(y)/dy}{m} \qquad (5)$$

$$\omega^2 = \frac{2k}{m}\left(1 - \frac{L_0}{d}\right) \qquad (6)$$

which shows that the frequency reduces as L_0 increases from small towards d. For a system with very taut springs, i.e. with $L_0 \ll d$ we find

$$\omega^2 = \frac{2k}{m} \qquad (7)$$

which if, of course, identical to the expression for longitudinal oscillations.

X.2.2 Small Displacement Approximation

In the case that $y \ll d$ we can apply a series expansion to the nonlinearity in the force equation and retain the leading term. We re-write eq.3 as

$$F = -2k\left[1 - \frac{L_0}{d}\left(1 + \frac{y^2}{d^2}\right)^{-1/2}\right]y$$

$$= -2k\left[1 - \frac{L_0}{d}\left(1 - \frac{1}{2}\frac{y^2}{d^2}\right)\right]y \quad (8)$$

which after some clearing up becomes

$$m\ddot{y} = -2k(d - L_0)\frac{y}{d} - kL_0\frac{y^3}{d^3} \qquad (9)$$

This expression, (which is an example of a *Duffing* equation), is interesting, since it describes the spring force as a sum of a linear term, and a cubic term in the non-dimensional variable y/d. The linear term of course agrees with eq.4.

Let us briefly look at the degree of approximation this equation affords us. Taking an engineering approach, the parameter d is assumed fixed. determined by the mechanical design. Then L_0 is a variable we can choose (depending on the selected spring). It's best to *non-dimensionalize* eq.4 by choosing L_0 as a fraction α of d, i.e., $L_0 = \alpha d$ which gives us

$$m\ddot{y} = -2k(1 - \alpha)y - k\alpha\frac{y^3}{d^2} \quad (10)$$

where we interpret α as selecting the weighting of the linear and non-linear terms, e.g. α close to 1 would select the nonlinear term and α close to 0 would select the nonlinear term. The ratio of nonlinear to linear terms is just

$$\frac{1}{2d^2}\frac{\alpha}{(1 - \alpha)} \qquad (11)$$

The plots in Fig.4 show the approximation to the force by eq.10 for $\alpha = 0.1$ and $\alpha = 0.9$.

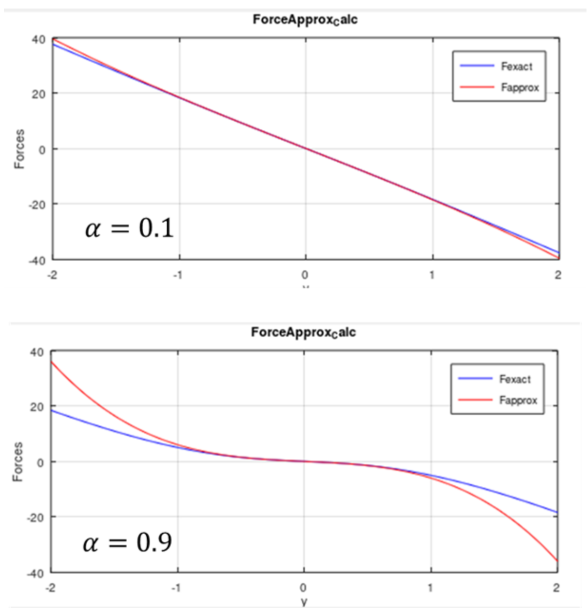

Figure 4. Variation of force with displacement for two values of α. Blue curves shown exact solution, eq.8, red curve approximation, from eq.10.

For the latter case, the error between full and approximate calculations of force at an amplitude of *d* is around 50%. Clearly we have to be careful with approximations.

X.2.3 Approximate Solution of the Nonlinear Equation

If we retained only the linear term in eq.9 then we know how to calculate the vibration frequency, and we know since the motion is harmonic, this frequency does not change with amplitude. The question is, how does the existence of the nonlinear term change this?

We are looking for a periodic solution to equ.X which suggests we should expand *y(t)* as a Fourier series and since we have a cubic term, this should include only the odd harmonics, so we try a solution of the form

$$y(t) \approx A\cos\omega t + B\sin 3\omega t$$

Then we equate all coefficients for terms involving $\cos\omega t$ and likewise for $\cos 3\omega t$. This process is called 'harmonic balance', the algebra is cumbersome and is provided as an appendix. The result is very informative, expressing frequency as a function of amplitude A of displacement we find

$$\omega^2 = \frac{2k}{m}\left(1 - \frac{L_0}{d}\right) + \frac{3k}{4m}\frac{L_0}{d^3}A^2 \qquad (12)$$

which may be written in the non-dimensionalized form

$$\omega^2 = \frac{2k}{m}(1-\alpha) + \frac{3k}{4m}\alpha\frac{A^2}{d^2} \qquad (13)$$

The first term is identical to equ.6 and the second reflects the nonlinearity. The effect of the nonlinearity is to increase the oscillation frequency, this is proportional to amplitude squared. This follows from the nature of the system force which increases with amplitude of deflexion.

Results for an experiment with $m = 0.5$, $k = 10$, $L_0 = 1$, $d = 1.5$ are shown in Fig.5. There is good agreement up to amplitudes around 30% of d.

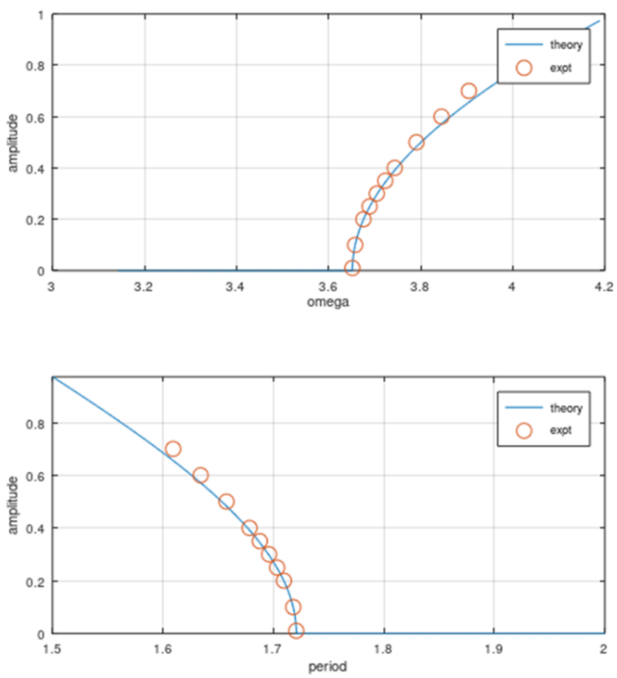

Figure 5. Theoretical predictions of amplitude against frequency with results of simulations.

These diagrams make sense, the frequency of oscillation increases with amplitude since the average force on the mass also increases with amplitude.

X.3 Unloaded Bistable Solution

X.3.1 Dynamical Equations and Oscillation Frequency

Here we are looking at the situation where $L_0 > d$ corresponding to Fig.6 where the springs start off under compression. The situation is sketched below. At the top the system has moved into equilibrium where the springs are uncompressed, so we have

$$L_0^2 = y_{equil}^2 + d^2 \qquad (14)$$

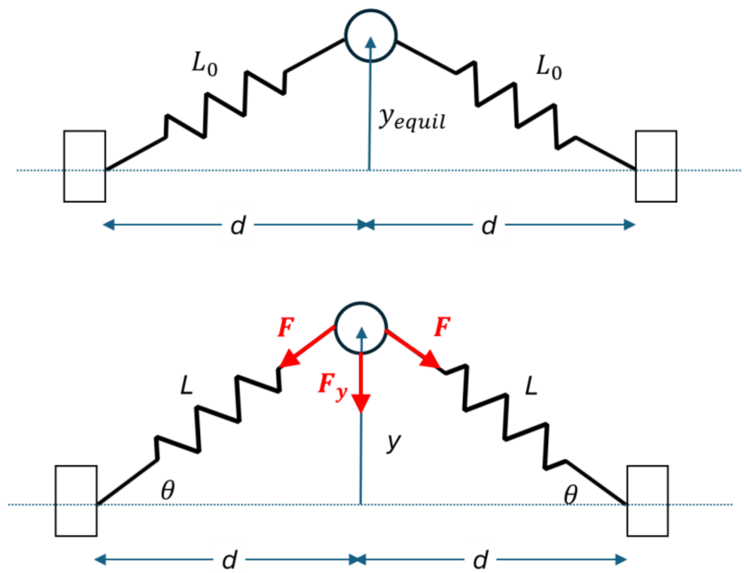

Figure 6. Bistable solution. The springs start off under compression, top shows the stable initial positions. Bottom shows the results of a displacement.

The mass is displaced upwards, and the restoring force is just

$$F(y) = -2k\left[1 - \frac{L_0}{(y^2 + d^2)^{1/2}}\right]y \quad (15)$$

To obtain the frequency of oscillation around y_{equil} we differentiate the force around this point,

$$\left.\frac{dF(y)}{dy}\right|_{y_{equil}} = -2k + 2k\frac{L_0}{(y_{equil}^2 + d^2)^{\frac{1}{2}}} - 2ky_{equil}^2\frac{L_0}{(y_{equil}^2 + d^2)^{\frac{3}{2}}} \quad (16)$$

$$= -2k\left(1 - \frac{d^2}{L_0^2}\right) \quad (17)$$

and we therefore have harmonic motion with

$$\omega^2 = \frac{2k}{m}\left(1 - \frac{d^2}{L_0^2}\right) \quad (18)$$

Note this is not the same as eq.6 for the monostable scenario.

Plots of the force, as a function of y and of its first derivative provide some useful information. The plots below correspond to the parameters m = 0.5kg, k = 10 N/m, d = 1.5m, L_0=2m.

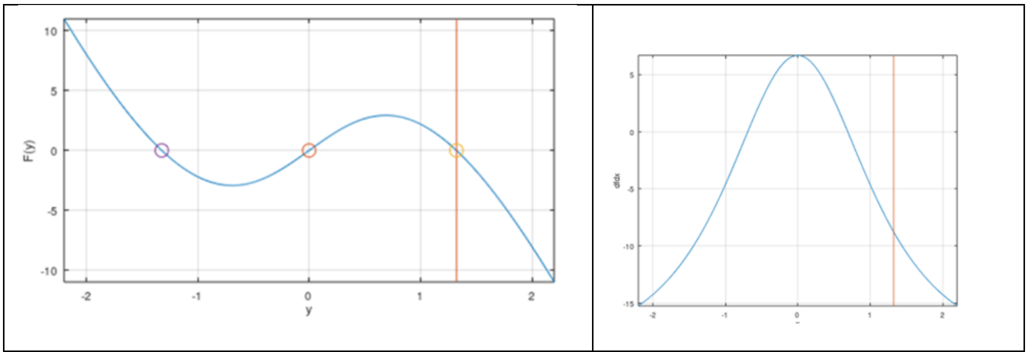

Figure 7. Restoring force (left) and first derivative (right) as a function of displacement *y*.

The force plot shows three equilibrium points; the stability of each can be tested by imagining a positive displacement about the point; for the right and left point, a positive displacement produces a negative restoring force, these points are stable. For the centre point a positive displacement produces a positive force which will drive the mass further from the unstable equilibrium value.

Let's look at how the force changes around the right stable equilibrium; it's clear to see that the force is always larger to the right of this point, therefore the oscillating mass will accelerate more in this rightmost region and so it's period of oscillation will decrease (if we agree that period smoothly changes with amplitude).

The system is bistable and symmetric, so the equilibrium solutions are

$$y_{equil} = \sqrt{L_0^2 - d^2} \qquad (19)$$

so, in the language of bifurcation theory, they appear as a 'pitchfork' bifurcation when we increase L_0 through d. This is shown together with some experimental results in Fig.8. The experimental system parameters were m = 0.5kg, k = 10 N/m, d = 1.5m.

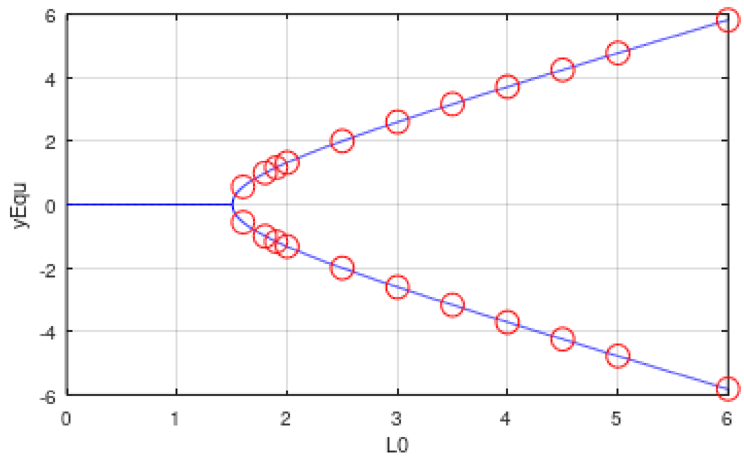

Figure 8. Bifurcation curve for y-equilibrium position as function of initial spring length. Curve from eq.19 simulated results shown as circles.

As we know, below $L_0 = d$ the equilibrium values are 0.

The periods of each experimental oscillation are shown in Fig.9 together with results obtained from eq.18.

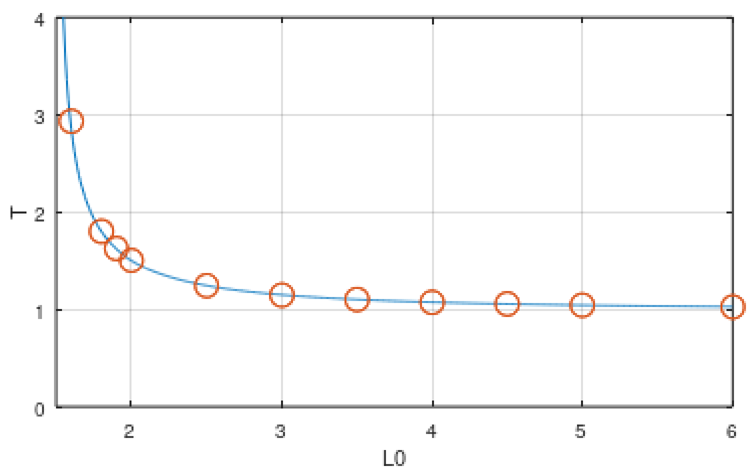

Figure 9. Variation of oscillation period with initial spring length. Curve from eq.18, simulation results shown as circles.

As predicted by eq.18 as L_0 approaches d the period rises sharply. This is because the restoring force hardly varies with displacement, the springs have effectively lost most of their stiffness. As L_0

increases eq.X reduces to $\omega^2 = 2k/m$ which for the given experimental values predicts a period of 0.994 seconds.

X.3.2 An Energy Approach

A complementary approach to understanding oscillations is to view the mass as moving in a potential well. We obtain the potential of our system

$$U(y) = -\int_0^y F(y)dy + cst \qquad (20)$$

which in this case evaluates to

$$U(y) = k\left[y^2 - 2L_0\sqrt{y^2 + d^2} - 2L_0 d\right] \qquad (21)$$

where we have chosen the constant of integration to set the PE zero at the bottom of the wells as shown in Fig.10. The equilibrium value of *y* is indicated. Note the assumption of zero friction.

Circles represent initial conditions for a few solutions, the displacements from y_{equ} are 0.1, 0.5, 0.66 and 0.7. The first three states have energies below the hump value so the mass will continue to oscillate trapped in the right potential well. The value of 0.7 has energy above the hump and so the mass will oscillate passing through both potential wells.

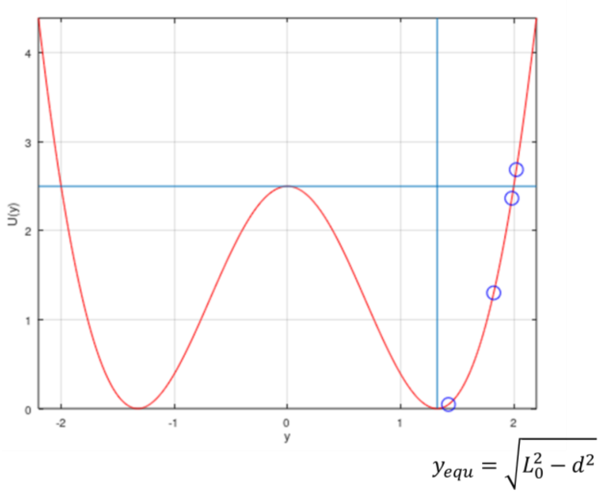

Figure 10. Graph of potential as function of displacement (from *y*=0) according to eq.21 with some possible starting locations showing three trapped and one 'free' trajectories.

Trajectories for these initial conditions are shown in Fig.11, on the left we have solutions trapped in the right well and on the right the solution traversing both wells.

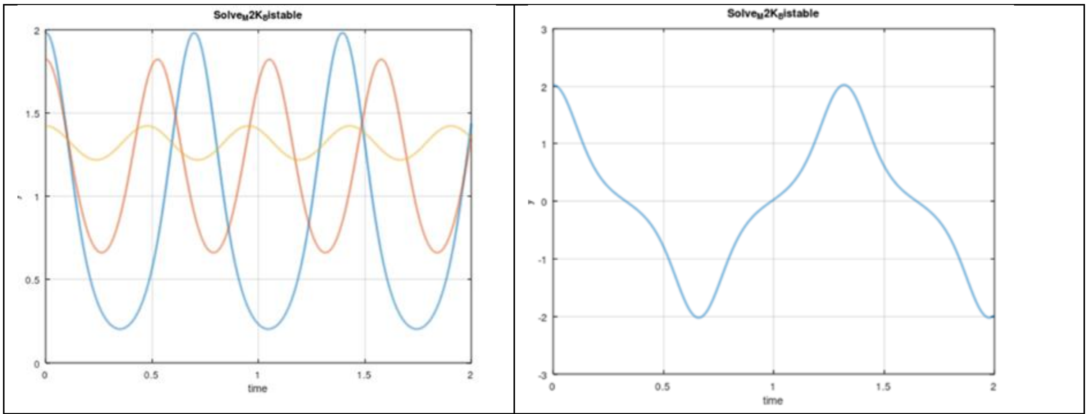

Figure 11. Trajectories of the system for the four initial conditions shown in Fig.10. Left shows the three 'bound' solutions, and right shows the 'free' solution.

We note that the form of the trajectories changes according to their initial conditions. For y=0.1 we obtain a low amplitude sine-like path. As the initial amplitude increases, the paths are deformed as the mass spends more time to the left of the equilibrium value due to the asymmetry of the potential curve; it needs longer to run up the shallower hill gradient than up the steeper gradient.

This agrees with the force discussion presented above.

X.4 Loaded Bistable Solution

X.4.1Dynamical Equations

Consider our M2K system, which is now located in the vertical plane, in this situation the mass will provide an additional downward force -mg, thus 'loading' the system. The diagram in Fig. 12 shows the system not in equilibrium

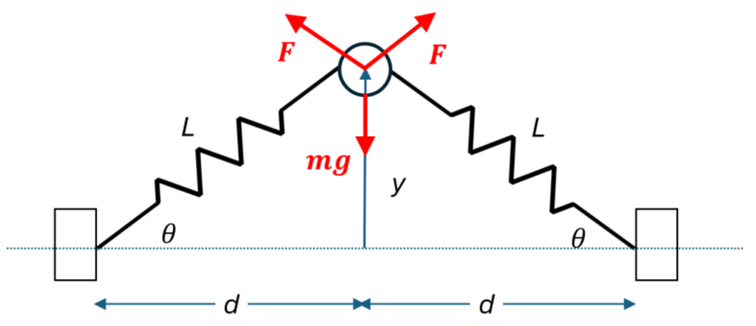

Figure 12. Bistable system located in a vertical plane taking the weight of the mass into account. Diagram shows forces for a displacement *y*.

Again we assume $L_0 > d$ so the springs starting off horizontal are under compression. The restoring force now becomes

$$F(y) = -2k\left[1 - \frac{L_0}{(y^2 + d^2)^{\frac{1}{2}}}\right]y - mg \qquad (22)$$

This force is now asymmetric about $y = 0$ as shown in the Fig.13, for out 'standard' loaded parameter set $m = 0.1$ kg, $d = 1.5$m, $k = 20$ N/m, and here with $L_0 = 2$.

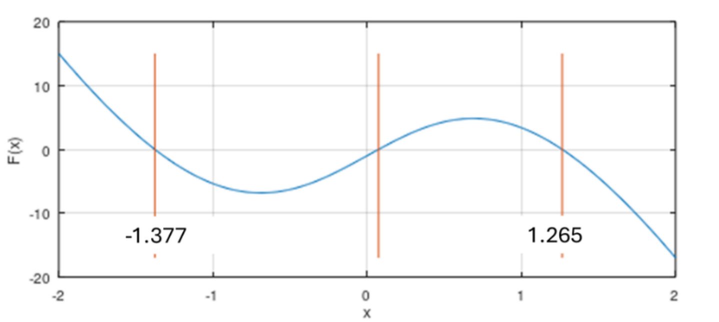

Figure 13. Force from eq.22 with equilibrium *y* values shown. Due to the load, the force curve is no longer symmetrical about *y*=0.

The equilibrium values of y, seen as a function of L_0 are lower than for the unloaded case as is expected, but the gradient of the force is the same. The frequency dependence will not be given by the simplified expression eq.18, since the equilibrium values are no longer given by $y_{equil} = \sqrt{L_0^2 - d^2}$, instead we must use the complete expression equ.16 and determine the equilibrium values numerically. When this is done we obtain the plot in Fig.14.

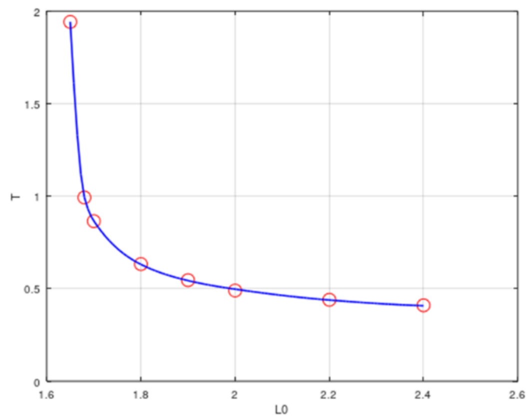

Figure 14. Plot of oscillation period against starting spring length. Curve generated using eq.16, circles show results of simulating the system ODEs.

There is clearly a critical value of L_0 (here just above 1.6) where the period rises rapidly. This will be explained below.

One may think that there is an additional solution type where the mass is in equilibrium below $y = 0$. Here, rather than starting under compression as assumed above, the springs could start in tension. This is shown in Fig.15 for the equilibrium situation.

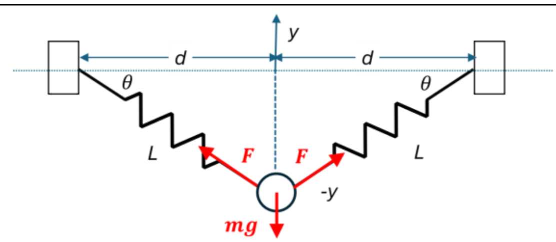

Fig.15 Proposed 'new' solution, the lower bistable configuration.

The springs still exert an upward force and at equilibrium the total force is zero

$$F = 0 = -2k\left[1 - \frac{L_0}{(y^2 + d^2)^{\frac{1}{2}}}\right] y - mg$$

where the spring force *appears* negative but remember in this expression $y < 0$. So this is not really a new solution since eq.(22) also includes this behaviour. When L_0 is used as the bifurcation parameter then $L_0 > d$ implies the spring initially in compression and $L_0 < d$ implies tension.

X.4.2 Bifurcation Equation

This equation results from searching for the equilibrium solutions to eq.(22),

$$\frac{mg}{2k} = \left[\frac{L_0}{(y^2 + d^2)^{1/2}} - 1\right] \qquad (23)$$

which can be solved *implicitly* (numerically) and is shown in Fig.16 as solid lines for the upper and lower branches.

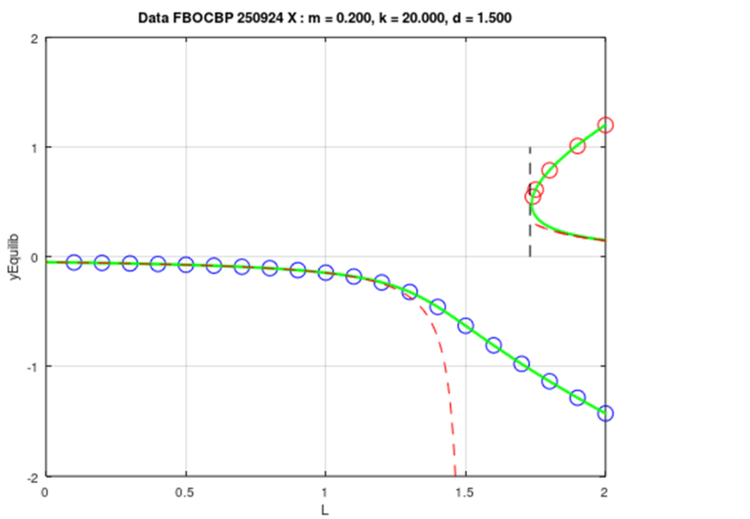

Figure 16. Bifurcation curve for equilibrium *y* from eq.23 with simulation results and approximation, equ.24.

Circles show experimental results for *m* = 0.2, *k* = 20, *d* = 1.5. While the solution from eq.(23) is exact, it is possible to obtain an approximate analytical expression for the equilibrium values. Using the condition $y < d$ a little algebra gives

$$y_{equ} = \left(\frac{mg}{2k}\right) \Big/ \left(\frac{L_0}{d} - 1\right) \qquad (24)$$

shown as red dashed lines in the above figure.

X.4.3 Bifurcation Unfolding

The effect of the loading is to skew the potential hill resulting in a shallower valley corresponding to the upper equilibrium point and a deeper lower valley. So if we started with a series of experiments with random distribution of initial conditions and added some damping to our system, more systems would come to rest at the bottom of the leftmost valley.

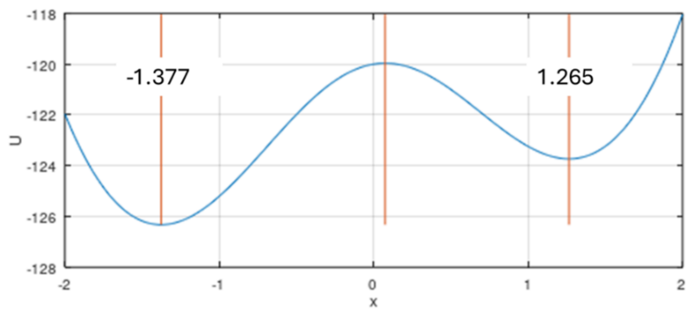

Figure 17. Potential hill representation of the problem

The shape of this well is sensitive to our key parameter L_0 and as this is reduced the springs become less stiff and we expect the valleys to become more shallow. We also expect a value of L_0 where the right valley disappears and so does the upper stable equilibrium point. We can explore this by plotting the potential as a function of both *x* and L_0 as shown in Fig.18..

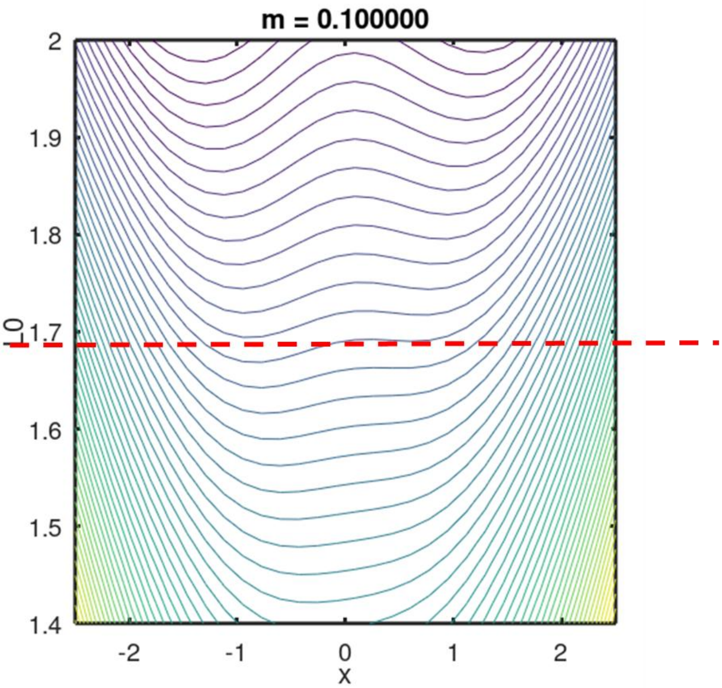

Potential curve as a function of both *y* and L_0. Red dotted line is an estimate of L_0 when the right valley just disappears.

As L_0 is reduced from 2.0 first the right valley disappears and then the left shifts its location to just under $x = 0$ which corresponds to the mass in equilibrium with the springs displaced downwards just enough to support its weight.

Of course we are interested in when the rightmost valley disappears; this can be done by inspection, the red dashed line suggest a value of L_0 just less than 1.7. The solution diagram for this value of L_0 is shown above.

X.4.4 The Period of Oscillations around Equilibrium

We are interested in what determines the period of oscillation of the mass when it is given a small nudge around its equilibrium position. An expression is directly derived from eq.(16), here for the frequency,

$$\omega^2 = \frac{2k}{m}\left[1 - \frac{L_0}{\left(y_{equ}^2 + d^2\right)^{1/2}} + \frac{y_{equ}^2 L_0^2}{\left(y_{equ}^2 + d^2\right)^{1/2}}\right] \quad (25)$$

where y_{equ} is the equilibrium position which must be calculated separately or obtained by experiment. We can obtain two analytical approximations to eq.(25).

First for small equilibrium value where $y_{equ} < d$ the second term in eq.(25) can be simplified and the third term ignored to give

$$\omega^2 = \frac{2k}{m}\left[1 - \frac{L_0}{d}\right] \quad (26)$$

These correspond to the mass located below the horizontal. Second when the springs start off compressed, and where $y_{equ}^2 + d^2 = L_0^2$ the first and second terms cancel and the third is simplified giving

$$\omega^2 = \frac{2k}{m}\left[1 - \frac{d^2}{L_0^2}\right] \quad (27)$$

These equations are plotted in Fig.19 together with experimental results for $m = 0.2$, $k = 20$, $d = 1.5$.

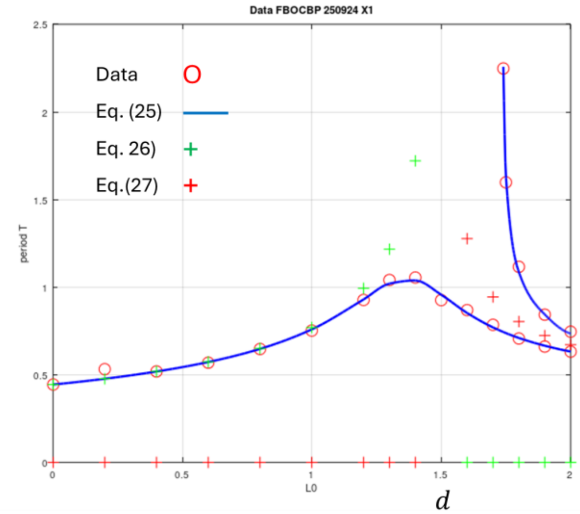

Figure 19. Plots of period against initial spring length L_0. Full and simplified theoretical solutions are plotted together with simulation data.

It's clear that eq.(26) provides a useful approximation over a good range of L_0 on the lower branch while the upper branch approximation has limited usefulness.

For completeness, we plot the periods against the observed equilibrium positions, Fig.20.

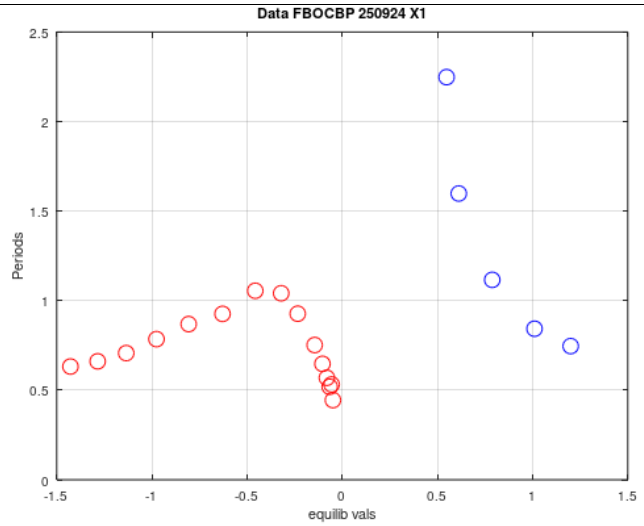

Figure 20. Plots of periods against equilibrium values. While solutions with any period appears possible, there is clearly a range of equilibrium values which is not.

It's evident that a range of equilibrium values between 0 and 0.5 were not realized experimentally. This is due to the unfolding of the bifurcation, see Fig.16 where a similar range is absent, and can be traced to the upper branch solutions jumping to the lower branch when the bifurcation parameter is reduced below a critical value. This *jump phenomenon* will be explored in Chapter.YY.